Kinetics and Free Energy Profiles of Spermine Transport in Liver Mitochondria†

Antonio Toninello,*,‡ Lisa Dalla Via,§ Roberto Stevanato,|| and Shiroki Yagisawa⊥

Dipartimento di Chimica Biologica, Università di Padova, and Centro di Studio delle Biomembrane del C.N.R. di Padova, Viale G. Colombo 3, 35121 Padova, Italy, Dipartimento di Scienze Farmaceutiche, Università di Padova, Via Marzolo 5, 35121 Padova, Italy, Dipartimento di Chimica Fisica, Università di Venezia, Calle Larga S. Marta 2137, 30123 Venezia, Italy, and School of Pharmaceutical Sciences, University of Nagasaki, 1-14 Bunkyo-Machi, Nagasaki, Japan 852

Received May 27, 1999; Revised Manuscript Received October 22, 1999

ABSTRACT: In the present study, the voltage-dependent mechanism of spermine transport in liver mitochondria [Toninello, A., Dalla Via, L., Siliprandi, D., and Garlid, K. D. (1992) *J. Biol. Chem. 267*, 18393−18397] was further characterized by determining the rate constants J_{max} and K_m as functions of membrane potential. An increase in mitochondrial membrane potential from 150 to 210 mV promoted spermine transport, as reflected by an approximate 4-fold increase in J_{max} and 25% decrease in K_m. The mechanism for the voltage dependence of transport was examined using the β value, i.e., the slope of ln(flux) vs $F\Delta\Psi/RT$ plots. Flux-voltage analyses performed at very high and very low spermine concentrations yielded β values of 0.125 and 0.25, for J_{max} and J_{max}/K_m, respectively. The physical significance of these β values was analyzed by means of a theory relating the enzyme reaction rate to the free energy profiles [Yagisawa, S. (1985) *Biochem. J. 303*, 305−311]. Depending on the nature of K_m, two possible models could be proposed to describe the location and shape of the barriers in the membrane. Analysis of previous data concerning spermine binding [Dalla Via, L., Di Noto, V., Siliprandi, D., and Toninello, A. (1996) *Biochim. Biophys. Acta 1284*, 247−252] by a new rationale provided evidence for an asymmetrical energy profile composed of two peaks with the binding site near the membrane surface followed by a rate-determining energy barrier for the movement of the bound spermine toward the internal region of the membrane.

The naturally occurring polyamines spermine, spermidine, and putrescine are transported into the matrix space of mitochondria by a specific, common uniporter system (*1*−*5*). This transport process is dependent on the membrane potential and exhibits a nonohmic flux−voltage relationship. It is insensitive to the pH of the medium, suggesting a strict electrophoretic behavior (*3*). Polyamine uptake is also temperature-dependent and increases with increasing charge number of the transported species, with an activation enthalpy of about 12 kJ/mol per charge at $\Delta\Psi$[1] ≈ 175 mV (*3*). These properties, combined with results obtained by flux−voltage analyses, suggest that the polyamine transporter is a saturable channel having two symmetrical energy barriers, with an energy well located in the middle of the membrane thickness (*3*).

Spermine that has accumulated in the mitochondrial matrix can be released at high constant proton−motive force by a pathway distinct from that of import, suggesting a continuous energy-dissipating influx−efflux cycling of the polyamine (*6*).

Due to the activity of the electrophoretic transporter, both spermine and spermidine are normally present in the inner compartment of liver mitochondria and are detectable in the isolated organelles (*7*). Many lines of evidence suggest that the presence of polyamines within the matrix plays an important physiological role in modulating energy metabolism. In this regard, given its stimulating effect on Ca^{2+} transport (*8*, *9*), it has been suggested that spermine stimulates the citric acid cycle by activating Ca^{2+}-dependent citrate synthase (*10*) and Ca^{2+}-dependent NAD-dehydrogenases (*11*−*14*). Other studies of energized mitochondria point to the ability of the polyamine to directly stimulate pyruvate dehydrogenase activity independent of its effect on Ca^{2+} transport (*15*).

Recently, by applying a new thermodynamic treatment of ligand−receptor interactions (*16*), mitochondrial membranes were found to possess two independent spermine-binding sites, both with monocoordination and low affinity/high binding capacity. These studies demonstrated that the binding of spermine to one of these sites, the so-called S_1 site, represents the preliminary step for spermine transport into the matrix (*17*). As previously reported, spermine is able to prevent the permeability transition in liver and heart mitochondria induced by different agents (*18*−*23*) (for reviews on the permeability transition see refs *24* and *25*). The binding site competent for this effect was found to be the above-mentioned S_1 site (*17*), thus suggesting a strict

† This work was supported by grants from the Ministero dell'Università e della Ricerca Scientifica e Tecnologica (MURST) and from the Consiglio Nazionale delle Ricerche (CNR).

* To whom correspondence should be adressed. Phone: (39) (49) 8276134. E-mail: toninell@civ.bio.unipd.it.

‡ Dipartimento di Chimica Biologica.

§ Dipartimento di Scienze Farmaceutiche.

|| Dipartimento di Chimica Fisica.

⊥ University of Nagasaki.

[1] Abbreviations: $\Delta\Psi$, electrical transmembrane potential; Hepes, 4-(2-hydroxyethyl)-1-piperazineethanesulfonic acid.

10.1021/bi991217c CCC: $19.00 © 2000 American Chemical Society
Published on Web 12/17/1999

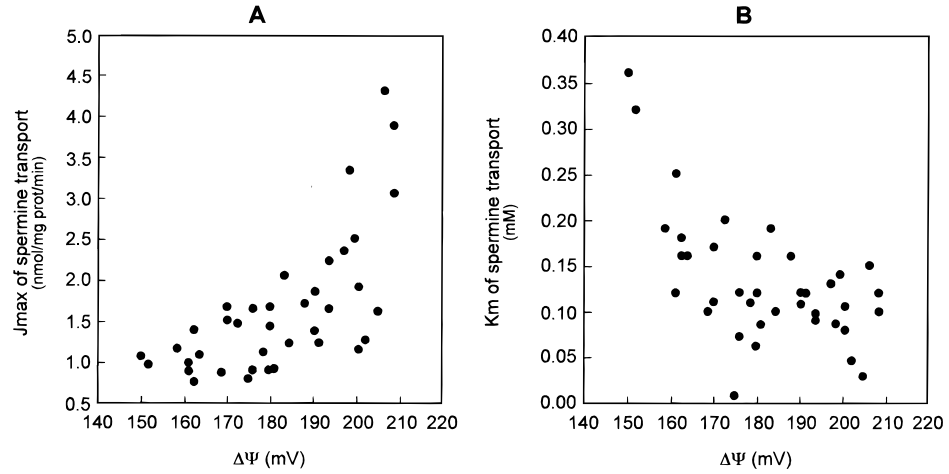

FIGURE 1: Variations in J_{max} (A) and K_m (B) for spermine transport in liver mitochondria as functions of the electric potential gradient. The initial rates of spermine transport were determined by incubating rat liver mitochondria in the presence of different concentrations of [^{14}C] spermine (10, 25, 50, 100, 250, and 500 μM and 1, 2.5, and 5 mM; 0.05 μCi/mL; see Experimental Procedures). The transport rates were linear with time during the incubation. The values of spermine uptake were corrected for the aliquots present in the extra-matrix space (*2*). Each J_{max} and K_m value calculated at a single $\Delta\Psi$ represents the mean of three determinations obtained from a daily mitochondrial preparation; $\Delta\Psi$ values in the range of 170−185 mV were obtained by assaying several preparations of mitochondria under normal conditions. $\Delta\Psi$ values below this range were obtained by adding limiting amounts (0−60 nM) of carbonyl cyanide *p*-trifluoromethoxyphenylhydrazone (FCCP). Higher $\Delta\Psi$ values were obtained by adding nigericin at different concentrations (0−330 nM).

correlation between spermine transport and its inhibition of the permeability transition.

A recent study found that this site exhibits diminished binding capacity and affinity upon depolarization (*26*). Under these conditions, both spermine uptake and protection against the permeability transition are compromised. This finding supports the hypothesis that spermine transport could participate in the regulation of the permeability transition, which, as very recently demonstrated, is involved in the pathway leading to apoptosis (*27*−*31*).

The aim of the present study was to further enhance our knowledge of the inward transport system. We examined the dependence of the rate constants on variations in membrane potential. The energy profiles for spermine transport were then evaluated on the basis of flux−voltage analyses (*3*) and a theory of enzyme kinetics related to free energy profiles (*32*).

EXPERIMENTAL PROCEDURES

Rat liver mitochondria were isolated in 250 mM sucrose and 5 mM Hepes (pH 7.4) by conventional differential centrifugation. The mitochondrial protein concentration was assayed by a biuret method with bovine serum albumin as a standard.

Incubations were carried out for 5 min at 20 °C with 1 mg of mitochondrial protein suspended in a low ionic strength medium, under conditions used in previous spermine transport studies (*1*−*3*). The medium contained 200 mM sucrose, 10 mM Hepes (pH 7.4), 5 mM succinate, 1.25 μM rotenone, and 1 mM phosphate. Sodium salts were used. Aliquots were taken at 1, 3, and 5 min and the uptake of [^{14}C]spermine was determined by a centrifugal filtration method as previously described (*1*−*3*). The concentrations of [^{14}C] spermine employed and further experimental details are provided in the legend to Figure 1.

Membrane potential ($\Delta\Psi$) was measured by using a selective electrode to monitor the distribution of the lipophilic cation tetraphenylphosphonium across the mitochondrial membrane (*33*, *34*) and corrected as previously proposed (*35*). Mitochondrial matrix volume was calculated from the distribution of [^{14}C]sucrose and ^3H_2O (*36*).

The kinetic constants were calculated by double reciprocal plots constructed from initial-rate measurements fitted to the Michaelis−Menten equation.

Rationale. (1) It is generally accepted that the theory describing ordinary enzyme kinetics can be applied to studies of ion transport across leaks and channels, provided that the phenomenon shows saturation behavior (*37*−*40*). Formally, the kinetics of transport through such ion pores are identical to simple enzyme kinetics and can be expressed by eq 1,

$$X + S_0 \underset{k_{-1}}{\overset{k_1}{\rightleftharpoons}} XS \xrightarrow{k_2} X + S_i \qquad (1)$$

where S_0 is the substrate (polyamine) at the outer side of the membrane, S_i is that at the inner side, X is a binding site in the channel, and XS is the substrate-binding site complex. In the absence of S_i, the rate of transport J is given by eq 2,

$$J = J_{max}[S]/(K_m + [S]) \qquad (2)$$

where J_{max} is the maximum rate at an infinitely high concentration of S_0 ([S]) and K_m corresponds to the Michaelis−Menten constant. The rate at an infinitely low concentration of S_0 is given by $J_{max}[S]/K_m$. As in ordinary enzyme kinetics, J_{max} is equal to k_2X_t, where X_t is the total concentration of the binding site, and K_m is equal to $(k_{-1} + k_2)/k_1$.

(2) As reported previously (*3*), the effect of electrical potential on the rate of spermine transport is expressed by eq 3,

$$J = J_0 \exp(z\beta F\Delta\Psi)/RT) \qquad (3)$$

where J_0 is the flux at $\Delta\Psi = 0$, z is the net charge of spermine and β is a parameter describing the effectiveness

of $\Delta\Psi$ in inducing transport and is related to the shape and position of the energy barrier (*3*, *40*).

The value of β is obtained from the slope of the ln J vs $F\Delta\Psi/RT$ plot and depends on the concentration of S. At [S] $\gg K_m$, the β value expresses the effect of $\Delta\Psi$ on J_{max} ($=k_2X_t$); at [S] $\ll K_m$, the β value expresses the effect of $\Delta\Psi$ on J_{max}/K_m [$=k_1k_2/(k_{-1} + k_2)$].

(3) The physical significance of the β values was analyzed by using free-energy profiles which were constructed by superimposing the applied electric potential. The resulting profiles were interpreted by using a theory that relates the reaction rate of enzymes to free-energy profiles (*32*). The two principles of the theory, which are described in further detail in the discussion, are (i) that the reaction rate is inversely proportional to the sum of the peak heights in the free-energy profiles measured from the level of all the preceding troughs, and (ii) that the effect of the substrate concentration on the transport rate can be represented by free-energy profiles depicting the real free-energy of the substrate in the form of eq 4,

$$G(X + S) = G^\circ(X) + G^\circ(S) + RT \ln[S] \qquad (4)$$

where $G^\circ(X)$ and $G^\circ(S)$ represent the free energies of the binding site and the substrate, respectively, at the standard state.

The present analysis dealt exclusively with spermine influx. Spermine efflux might be predicted to affect the experimental data and their interpretation for two reasons. First, the efflux of the imported labeled spermine would directly decrease the amount measured as influx (the subject of the present theoretical analysis). Second, use of the same channel for influx and efflux might result in a phenomenon resembling product inhibition. Liver mitochondria are reported to contain an intrinsic spermine concentration of 3−5 mM (*7*); therefore, the first possibility is excluded by the fact that when liver mitochondria are charged with 1 mM external spermine, the steady-state internal concentration reaches about 60 mM (*2*). This means that at 60 mM the efflux of the internal spermine becomes comparable to the influx of less than 1 mM external spermine. Therefore, the efflux of imported labeled spermine was negligible in the kinetics assays, which were carried out in the first 5 min of incubation, with external spermine at around 1 mM, resulting in lower levels of accumulated spermine. Furthermore, it is also to be taken into account that the main process of spermine export, which is driven by a ΔpH-dependent symporter (cotransport with phosphate) (*6*) and thus differs from the reverse of the $\Delta\Psi$-dependent electrophoretic uniporter of the present study, is triggered after several minutes of incubation and takes place when a substantial amount of the polyamine has already accumulated and ΔpH has reached a critical threshold value (Toninello, A., Dalla Via, L., Di Noto, V., and Yagisawa, S., unpublished results). The possibility of product inhibition is also unlikely, because, as noted above, spermine is mainly exported by a mechanism distinct from the reverse of the present electrophoretic process; thus, product inhibition related to export cannot occur. On the basis of these considerations, spermine efflux was not taken into account in present analysis. Furthermore, the intrinsic rate of the reverse of the present $\Delta\Psi$-dependent electrophoretic process is very slow, as shown in the following calculation. At equilibrium, the concentrations of spermine at both sides of the membrane should obey the equation: $[S]_i = [S]_o \exp(zF\Delta\Psi/RT)$, where $[S]_i$ and $[S]_o$ denote the concentrations (activities) at both sides. For $z = +4$ and $\Delta\Psi = 180$ mV, the equation gives a value of 10^{12} for the ratio of $[S]_i/[S]_o$. The observed steady-state concentration ratio (60 mM/1 mM) is much lower than this, indicating that the spermine concentration is kept low by an energy-linked efflux process. The ratio of $[S]_i/[S]_o$ at equilibrium also gives the rate constant for spermine efflux by the reverse of the present electrophoretic mechanism, i.e., 10^{-12} of the influx rate constant; it is unlikely that this miniscule rate constant has any effect on the process.

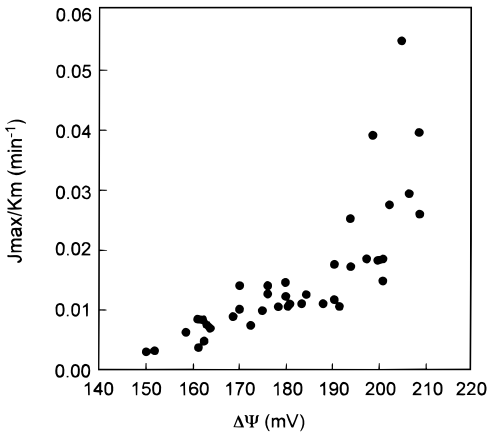

FIGURE 2: Variations in J_{max}/K_m as a function of the electrical potential gradient. The values of J_{max} and K_m were derived from the results reported in Figure 1.

RESULTS

The results reported in Figure 1 show the variations in both J_{max} and K_m for spermine transport, as a function of $\Delta\Psi$, evaluated in the range of about 150−210 mV. The fluctuations in the experimental data shown in this and subsequent figures are very probably due to variations in the different mitochondrial preparations utilized, as described in the legend to Figure 1. The points reported in the diagrams suggest an exponential trend for both constants. J_{max} increases with $\Delta\Psi$ by about 4-fold (from about 1 to 4 nmol mg protein^{-1} min^{-1}; Figure 1A); K_m diminishes by the same increment over this $\Delta\Psi$ range (from about 0.4 to 0.1 mM; Figure 1B).

Figure 2 shows the variations in the J_{max}/K_m ratio as a function of $\Delta\Psi$. The resulting plot also suggests an exponential trend for this parameter, as observed for J_{max} in Figure 1A. The calculations demonstrate that when $\Delta\Psi$ is increased from 150 to 210 mV, J_{max}/K_m increases by more than 1 order of magnitude (about 16-fold).

Figure 3 reports the variations in both ln J_{max} and ln J_{max}/K_m as a function of $F\Delta\Psi/RT$. As described previously (*3*), this representation of the data is referred to as flux/voltage analysis. The relationship between ln J_{max} and $F\Delta\Psi/RT$, corresponding to saturation conditions (see point 2 of Rationale), shows considerable scatter, but is probably linear (Figure 3A). The straight line obtained in the diagram (linear regression coefficient = 0.75) exhibits a slope = 0.5, yielding a β value of 0.125, with $z \simeq 4$, at pH 7.4. The relationship between ln J_{max}/K_m and $F\Delta\Psi/RT$, corresponding to low

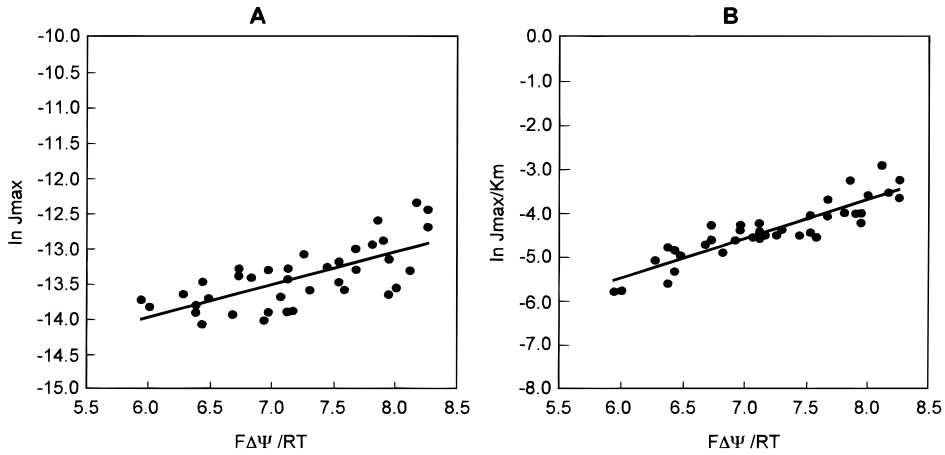

FIGURE 3: Rate constant/voltage analyses of spermine transport. Shown are log-linear plots of J_{max} (A) and J_{max}/K_m (B) derived from the data reported in Figures 1A and 2 according to the rationale proposed in the text. Linear regression yielded values for the slopes of the curves that represent the product zβ (see eq 2). Regression coefficient = 0.75 in panel A and 0.93 in panel B.

spermine concentrations (point 2 of the rationale), clearly shows a linear trend, with a slope = 1 and $\beta = 0.25$ (Figure 3B). It is noteworthy that calculation of ln J_{max}/K_m dramatically reduces the scattering observed in the diagrams in Figures 1A and 2. The resulting straight line has a good linear regression coefficient (0.93).

The β for K_m defined by eq 5, where $K_{m,0}$ is the K_m value at $\Delta\Psi = 0$, can be obtained from the slope in the plot of ln K_m vs $\Delta\Psi$. The β value can also be calculated from eq 6, which is derived by dividing eq 7 by eq 8.

$$K_m = K_{m,0} \exp[\beta(K_m)zF\Delta\Psi/RT) \quad (5)$$

$$\beta(K_m) = \beta(J_{max}) - \beta(J_{max}/K_m) \quad (6)$$

$$J_{max} = J_{max,0} \exp[\beta(J_{max})zF\Delta\Psi/RT] \quad (7)$$

$$J_{max}/K_m = (J_{max}/K_m)_0 \exp[\beta(J_{max}/K_m)zF\Delta\Psi/RT] \quad (8)$$

On the basis of the calculated $\beta(J_{max}) = 0.125$ and $\beta(J_{max}/K_m) = 0.25$, these equations yield a $\beta(K_m)$ value of -0.125. The negative value reflects the decrease in K_m as $\Delta\Psi$ is increased.

DISCUSSION

The results reported in this paper point out a peculiar aspect of spermine transport in liver mitochondria, i.e., the strict dependence of both K_m and J_{max} on the electrical transmembrane potential. By taking into account previous results demonstrating that the rate of spermine transport is exponentially dependent on $\Delta\Psi$ (*2*, *3*), it is realistic to expect that J_{max} also increases exponentially as $\Delta\Psi$ is raised, as observed experimentally in Figure 1A. However, a new aspect of this kinetics is evident from the results reported in Figure 1B, which show that K_m is also sensitive to $\Delta\Psi$, and decreases exponentially as $\Delta\Psi$ is raised. The combined effect is shown in the steeper trend of the experimental points obtained by plotting J_{max}/K_m vs $\Delta\Psi$ (Figure 2).

The physical significance of these phenomena can be discussed most rationally by using the β values, which are related to the shape and position of the energy barriers in the ion transport pathway (*40*). Indeed, in a previous report, a reaction model consisting of two barriers symmetrically spaced across the membrane was deduced from the β value measured at a single substrate concentration (*3*). The present results indicate that this model should actually consist of two peaks asymmetrically located across the membrane (see below).

In the present analysis, Eyring-type barriers were assumed for the kinetic steps. Alternatively, membrane permeation of ions can be analyzed using the electrodiffusive description of the Nernst−Planck theory. When extended to account for the presence of binding sites (*42*), this theory is applicable to the present case, in which the presence of a specific binding site was exhibited by competitive inhibition by polyamines (*3*). The basic equations of the extended theory giving the voltage dependence of kinetic steps are quite similar to the Eyring equation. The two models differ only in the values of preexponential factors and the presence of a function named the shape function in the Nernst−Planck model, which represents the deviation of the rate constants from the simple exponential voltage dependence (*42*). Therefore, with the exception of the absolute values of the activation energy, the present theoretical conclusions are also consistent with the Nernst−Planck-type theory, provided that sharp barriers are assumed for the transport process. At present, the available experimental information does not allow determination of the shape function.

Principle Underlying the Theoretical Treatment. Figure 4 shows the free-energy profiles representing eq 1, modified by the transmembrane electric potential, which changes linearly across the membrane. These free-energy profiles, as well as those in Figures 5 and 7, were fitted to a two-barrier, one-site model with asymmetric peaks. The electric potential energy was simply superimposed on the free-energy profiles based on the assumption that the transport process occurs principally by diffusion and is not associated with special movements of the channel protein. Therefore, the peaks and troughs in the free-energy profiles can be correlated to the real barriers and wells in the membrane, where the free energy of the substrate ion is affected by the local electric potential according to simple electrostatics (z$F\Psi$). According to the transition-state theory, the rate constant represented by a peak in the free energy profile is proportional to the ratio of the equilibrium substrate concentrations present at the bottom of the preceding well and

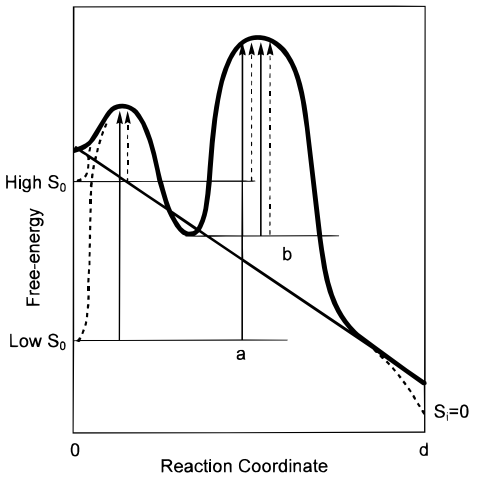

FIGURE 4: Free-energy profiles modified by transmembrane potential; effect of the substrate concentration. The bold line represents the energy profile modified by a linear electric potential for the standard state, when the substrate concentrations outside and inside the membrane, i.e., S_o and S_i, respectively, are both considered 1 M by convention. The dotted lines show the modification of the profile in the presence of the same electric potential when $S_i = 0$ and S_o is either low or high. As explained in the text, the arrows represent the components contributing to the transport rate.

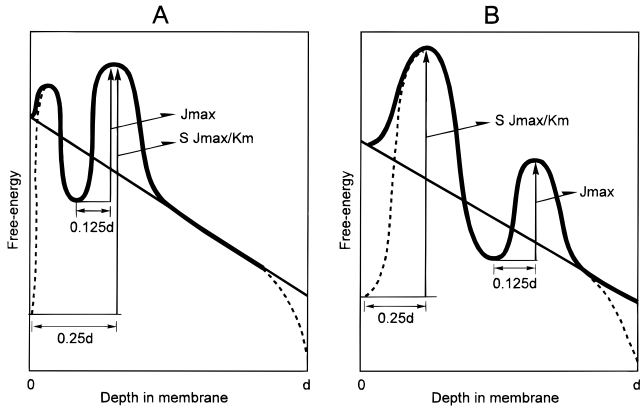

FIGURE 5: Interpretation of the β values in the free energy profiles. Shown are the profile for the case of $K_m = k_{-1}/k_1$ and the case of $K_m = k_2/k_1$ (plots A and B, respectively). The numbers associated with *d* indicate the fractional distance in reference to the total membrane thickness (*d*).

at the top of the peak. Therefore, the rate constant represented by a peak is modulated by the electric potential by the factor $\exp[-(\Psi_t - \Psi_w)zF/RT]$, where Ψ_t and Ψ_w are the electric potential at the top of the peak and at the bottom of the well, respectively. These considerations lead to an important conclusion: the β value for the rate constant equals the ratio of $\Psi_t - \Psi_w$ to transmembrane potential $\Delta\Psi$. In other words, the β value, given by $\Psi_t - \Psi_w$, indicates the lateral distance between the peak apex and the bottom of the well if a linear electric potential is assumed. Examples are shown in later figures.

Figure 4 also shows the free-energy profile of transport at different substrate concentrations. As noted in point 3 of Rationale, the transport rate is inversely proportional to the sum of the peak heights (indicated by arrows in the figure). In an approximate treatment, the transport rate is given by the largest peak height, indicated by the longest arrow in the figure; the rates at the lowest and highest substrate

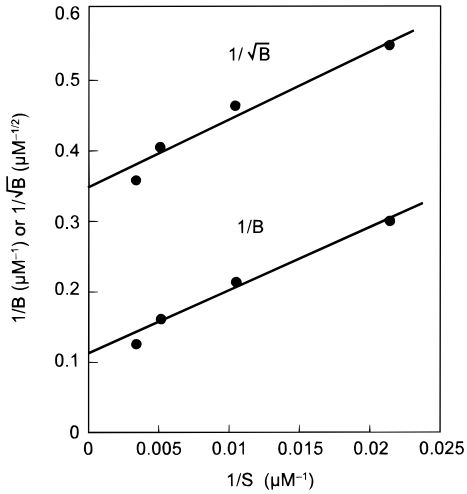

FIGURE 6: Two types of double reciprocal plots for spermine binding by mitochondria. Spermine-binding data reported in ref *17* obtained at substrate concentrations similar to those used in the present measurements were plotted according to eqs 10 and 12. The K_m value obtained by the least-squares method is 0.085 mM for the $1/B$ versus $1/S$ plot, and 0.029 mM for the $1/\sqrt{B}$ versus $1/S$ plot. The significance of the plot of $1/\sqrt{B}$ versus $1/S$ is given in the text.

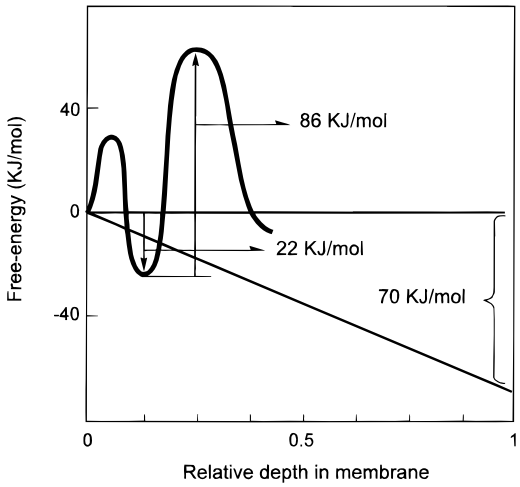

FIGURE 7: Free energy of the spermine transport channel at 180 mV. The height of the first peak is not known; the height of the second peak was calculated from J_{max} per milligram of protein by use of the transition state theory and the number of high-affinity binding sites per milligram of protein determined in a previous report (*17*). The depth of the well for the binding site was calculated from the K_m value at 180 mV.

concentrations are indicated by arrows a and b, respectively. These arrows correspond to $J_{max}[S]/K_m$ and J_{max}, respectively and identify the wells and peaks to be referred to when considering the effect of $\Delta\Psi$ described above.

In the above discussion, spermine was assumed to have full charge of +4 during transport. However, spermine might be transported as a partially neutralized ion pair, resulting in lower β values. One could propose that the moderately neutralized ion would be more likely to move into hydrophobic region of the membrane, although the electrostatic motive force is reduced by the decreased net positive charge. This possibility is refuted by several lines of evidence. First, the transport rate of polyamines is known to greatly increase with increasing charge (i.e., spermine > spermidine > putrescine), indicating that more highly charged species are

more readily transported (*3*). Furthermore, the nearly identical β values measured for these polyamines, which are transported by the same channel as judged from their mutual competitive inhibition (*3*), strongly suggest that the β values reflect a common structural feature of the transport channel. It should also be noted that the temporary neutralization of the net charge of spermine, for example, by binding to an anionic binding site does not affect its β value, provided that the tetravalent form represents the only transported species. This is because the changes in electrostatic energy due to charge neutralization are already built into the original energy profiles in the absence of the transmembrane potential. The transmembrane potential independently increases the electrostatic energy of the spermine ion by the value of $4F\Psi$; thus, the β value is not affected by temporary neutralization.

Interpretation of Experimental β Values. As in ordinary enzyme kinetics, two extreme cases of K_m, namely $K_m = k_{-1}/k_1$ and $K_m = k_2/k_1$, will be considered. Figure 5 shows the free-energy profiles for these K_m values at the lowest and highest substrate concentrations. For the purpose of discussion, we will refer to the first and second peaks in these profiles as the k_1 and k_2 peak, respectively.

On the basis of the analyses described above, it becomes apparent that in both cases of K_m, the β value of 0.125 measured at J_{max} corresponds to the relative lateral distance between the well for binding site XS and the top of the k_2 peak. In the case of $K_m = k_{-1}/k_1$, the β value of 0.25 measured at J_{max}/K_m can be assumed to correspond to the distance between the membrane surface and the top of the k_2 peak (Figure 5A). When $K_m = k_2/k_1$ (Figure 5B), the β value of 0.25 corresponds to the distance between the membrane surface and the top of the k_1 peak. A notable difference between the two cases of K_m is that the β values determine the location of the binding site XS when $K_m = k_{-1}/k_1$, but not when $K_m = k_2/k_1$.

The argument regarding the location of the binding site and the energy barriers is based on the assumption that the electric potential remains linear across the membrane. However, even if this is not the case, the argument will not be seriously flawed as long as the potential changes monotonically and without inversion.

Generally, the abscissa should be taken as the distance corrected for the electric field. For example, in the case of $K_m = k_{-1}/k_1$, the binding site is located at the position corresponding to 1/8 of the total membrane potential.

Discrimination of the Two Cases of K_m. As shown in the preceding section, discrimination of the two cases of K_m is of critical importance for understanding the reaction mechanism. The property of K_m expressed as $(k_{-1} + k_2)/k_1$ is determined by the relative values of k_{-1} and k_2. In enzyme reactions, the first step, usually concerned with formation or breakdown of noncovalent bonds, is much faster than the second step, which involves rearrangement of covalent bonds; thus, $K_m = k_{-1}/k_1$ is the rational assumption in most cases. On the contrary, in transport processes, both steps are noncovalent and there is no proper rationale for discriminating the two cases of K_m. In the present case, k_{-1} corresponds to the movements of spermine from the substrate-binding site (XS) toward the outer part of the membrane, where a higher dielectric constant is expected, and k_2 corresponds to the movements of the polyamine toward the inner part of the membrane, where a lower dielectric constant is expected. Thus, considering the ionic character of the substrate, $k_{-1} > k_2$ can be assumed; however, the magnitude of the difference is not clear. Furthermore, the presence of a high membrane potential must facilitate the k_2 step but retard the k_{-1} step, thus favoring the case of $K_m = k_2/k_1$. This can be seen from energy profiles in which k_2 and k_{-1} are represented by the barriers before and after the well of the XS complex, respectively; an increase in the slope of the electric potential decreases the height of the barrier representing k_2 but increases the height of the barrier representing k_{-1}. As stated above, there is no simple rationale for discriminating the two cases of K_m.

Therefore, we developed a new method to solve this problem. Evidence supporting the case of $K_m = k_{-1}/k_1$ was provided by an analysis of data from a previous study concerning binding of spermine to mitochondria (*17*) that used a different experimental approach and rationale: spermine uptake by mitochondria was measured during the first 5 min, and the spermine bound to the mitochondrial membrane was calculated by extrapolating the time course back to zero time. The data were analyzed with the implicit assumption of quasi-equilibrum for the binding step, namely under the condition of $K_m = k_{-1}/k_1$. The present study extends this analysis to the case of $K_m = (k_{-1} + k_2)/k_1$.

In the process described by eq 1, XS + S_i, i.e., the sum of spermine bound to the membrane and that already imported, gives the amount of spermine taken up by mitochondria. This value generally changes in a time course, exhibiting an initial rapid increase followed by a linear increase corresponding to the steady-state rate. The burst size, i.e., the intercept on the vertical axis obtained by interpolating the linear portion to zero time, is given by eq 9,

$$B = \frac{X_t}{1 + K_m/S_o} - \frac{k_2 X_t}{k_1 S_o (1 + K_m/S_o)^2} \tag{9}$$

where X_t denotes the total concentration of binding sites. This corresponds to the amount of membrane-bound spermine determined in the previous experiment (*17*). Equation 9 was derived from a formula describing the time course of S_i solved for an equivalent process in enzyme kinetics (*41*). Equation 9 becomes eq 10 when $K_m = k_{-1}/k_1$ and becomes eq 11

$$B = \frac{X_t}{1 + K_m/S_o} \tag{10}$$

$$B = \frac{X_t}{(1 + K_m/S_o)^2} \tag{11}$$

when $K_m = k_2/k_1$. Equation 10 indicates that, when $K_m = k_{-1}/k_1$, B is equal to the concentration of XS at steady state and can be treated as ordinary binding data; eq 11 indicates that this is not the case when $K_m = k_2/k_1$. Equations similar to eq 11 have been used in active-site titration of enzymes. The difference between eqs 10 and 11 reflects the presence of a lag phase in the time course of S_i under the condition of $K_m = k_2/k_1$. Equation 12 is derived from eq 11 and indicates

$$\sqrt{B} = \frac{\sqrt{X_t}}{(1 + K_m/S_o)} \tag{12}$$

that, in the case of $K_m = k_2/k_1$, $\sqrt{B}$ can be treated by standard procedures such as Scatchard plot and double reciprocal plot. Figure 6 shows double reciprocal plots based on eqs 10 and 12. The data analyzed in these plots were obtained in previous experiments (*3*) using mitochondria preparations with a membrane potential of 175−185 mV. Of the data reported, we used only those obtained at spermine concentrations of 50−300 μM, similar to the concentration range used in the present kinetic measurements. The two plots in Figure 6 show similar linearity, and it is difficult to ascertain which plot is better fitting. However, the K_m value of 0.085 mM calculated from the ordinary plot based on eq 10 is close to the K_m kinetically determined in the present experiment (i.e., 0.12 mM at 180 mV). The K_m from the square root plot based on eq 12 is 0.029 mM, significantly smaller than the experimental value. Therefore, the binding data support the case of $K_m = k_{-1}/k_1$.

Properties of the Spermine Binding Site. The above discussion supports the case of $K_m = k_{-1}/k_1$ and the energy profile depicted in Figure 5A. In this reaction model, spermine binds to a binding site placed near the surface of the membrane; the bound spermine is in rapid equilibrium with external spermine, and the k_2 step, i.e., the movement of spermine toward the inner part of the membrane, is the rate-limiting step. Figure 7 shows the free-energy profile of the system with numerical values at a membrane potential of 180 mV. The height of the k_2 peak was calculated from the J_{max} per milligram of protein and the number of high-affinity binding sites (∼8 nmol/mg of protein) determined in a previous study (*17*). No information is available for the height of the k_1 peak. The potential difference of 180 mV corresponds to 70 kJ/mol, taking into account the valency of spermine. The perturbation by the potential difference corresponding to the β value of 0.125 is about 9 kJ/mol (70 × 0.125). The energy barrier for the k_2 step has a steep ascending limb corresponding to the small β. This can be interpreted as evidence for the presence of a discrete spermine-binding site. This site is consistent with the small K_m value and with strict competitive inhibition exhibited by spermidine and putrescine for spermine transport (*3*). Discrimination of the shape of the energy barriers is an important step in the elucidation of transport processes and broad energy barriers are also assumed in some cases (*42*). A fact to be noted concerning this problem is that kinetic data tell nothing about the energy barriers behind the rate-determining step, that is the k_2 peak in the present case. What is certain is that the peaks and wells in the profile match the experimental observations made for the transport system. In this respect, analysis of the reverse flow of spermine would be quite interesting, and is expected to give information concerning the situation behind the k_2 peak. This measurement will confirm the location of the rate-determining barrier, which must be the same for transport in both directions due to the law of energy conservation. It also might explain the presence of a binding site on the other side of the membrane. However, unfortunately such an analysis is not possible in the present case because spermine is exported mainly by a distinct mechanism. The problem concerning the ambiguity in the energy profile will be discussed in the following section.

General Applications of Free Energy Profiles for the Analysis of Transport Processes. It seems appropriate to make some comments regarding the general utility of the present procedure for the analysis of transport processes. Ion transport by channels has been analyzed by various approaches based on a variety of models (*42*). Membrane models with symmetric energy profiles have been used in many cases. In some studies, transport has been treated as a stochastic process governed by transport probabilities (*42*, *43*). Despite these differences, the present procedure is applicable to various models so long as the processes can be expressed in the form of free-energy profiles. In this respect, it is worth noting that most stochastic formalisms are mathematically equivalent to ordinary kinetic formulas in the sense that they use the solutions of a set of differential equations exhibiting individual steps solved under similar limiting conditions. The restrictions in the application of the present method are that the transport should be unidirectional and does not involve reverse flow and that only one ion molecule can occupy the channel; these restrictions arise from the limits in the original theory (*32*). However, transport involving reverse flow and analyses of the effects of inhibitors can be examined by extending the present method according to the original theory.

In conclusion, the principal feature of the spermine transport system has been clarified on the basis of the membrane-potential dependence of J_{max}/K_m and J_{max} by use of two theoretical procedures. The transport system is composed of a binding site near the membrane surface, with spermine bound to the site in rapid equilibrium with the external spermine. Further analysis of the process will require additional information, especially at the structural level. Nevertheless, both kinetic and thermodynamic information, along with the data analysis procedures such as one developed in the present study, are equally important for the elucidation of transport dynamics.

ACKNOWLEDGMENT

The authors wish to thank Prof. Ferdinando Palmieri (Dipartimento Farmaco-Biologico, Università di Bari) and Prof. Keith D. Garlid (Oregon Graduate Institute of Science and Technology, Portland, OR) for helpful discussions and suggestions. The authors are also grateful to Mr. Mario Mancon for his skillful technical assistance and to Mrs. Flavia Bergamin and Mr. Giovanni Di Falco for their secretarial work.

REFERENCES

1. Toninello, A., Di Lisa, F., Siliprandi, D., and Siliprandi N. (1985) *Biochim. Biophys. Acta 815*, 399−404.
2. Toninello, A., Miotto, G., Siliprandi, D., Siliprandi, N., and Garlid, K. D. (1988) *J. Biol. Chem. 263*, 19407−19411.
3. Toninello, A., Dalla Via, L., Siliprandi, D., and Garlid, K. D. (1992) *J. Biol. Chem. 267*, 18393−18397.
4. Toninello, A., Dalla Via, L., Testa, S., Siliprandi, D., Siliprandi, N. (1990) *Cardioscience 1*, 287−294.
5. Tassani, V., Ciman, M., Sartorelli, L., Toninello, A., and Siliprandi, D. (1995) *Neurosci. Res. Commun. 16*, 11−18.
6. Siliprandi, D., Toninello, A., and Dalla Via, L. (1992) *Biochim. Biophys. Acta 1102*, 62−66.
7. Tassani, V., Campagnolo, M., Toninello, A., Siliprandi, D. (1996) *Biochem. Biophys. Res. Commun. 226*, 850−854.
8. Denton, R. M., and McCormack, J. G. (1980) *FEBS Lett. 119*, 1−8.
9. Nicchitta, C. V., and Williamson, J. R. (1984) *J. Biol. Chem. 259*, 12978−12983.

10. Yoshino, M., Yamada, Y., and Murakami, K. (1991) *Biochim. Biophys. Acta 1073*, 200−202.
11. McCormack, J. G. (1989) *Biochem. J. 264*, 167−174.
12. Damuni, Z., and Reed, L. J. (1987) *J. Biol. Chem. 262*, 5133−5138.
13. Kiechle, F. L., Malinski, H., Dandurand, D. M., and McGill, J. B. (1990) *Mol. Cell. Biochem. 93*, 195−206.
14. Rutter, G. A., Diggle, T. A., and Denton, R. M. (1992) *Biochem. J. 285*, 435−439.
15. Tassani, V., Cattapan, F., Siliprandi, D., and Toninello, A. (1995) *It. J. Biochem. 44*, 61A−62A.
16. Di Noto, V., Dalla Via, L., Toninello, A., Vidali, M. (1996) *Macromol. Theory Simul. 5*, 165−181.
17. Dalla Via, L., Di Noto, V., Siliprandi, D., and Toninello, A. (1996) *Biochim. Biophys. Acta 1284*, 247−252.
18. Siliprandi, N., Siliprandi, D., Toninello, A., and Garlid, K. D. (1988) in *Molecular Basis of Biomembrane Transport* (Palmieri, F., and Quagliariello, E., Ed.) pp 155−162, Elsevier, Amsterdam.
19. Lapidus, R. G., and Sokolove, P. M. (1993*) Arch. Biochem. Biophys. 306*, 246−253.
20. Rigobello, M. P., Toninello, A., Siliprandi, D., Bindoli, A. (1993) *Biochem. Biophys. Res. Commun. 194*, 1276−1281.
21. Lapidus, R. G., and Sokolove, P. M. (1994) *J. Biol. Chem. 269*, 18931−18936.
22. Tassani, V., Biban, C., Toninello, A., and Siliprandi, D. (1995) *Biochem. Biophys. Res. Commun. 207*, 661−667.
23. Lapidus, R. G., and Sokolove, P. M. (1992) *FEBS Lett. 313*, 314−318.
24. Gunter, T. E., and Pfeiffer, D. R. (1990) *Am. J. Physiol. 258*, C775−C786.
25. Zoratti, M., and Szabo, I. (1995) *Biochim. Biophys. Acta 1241*, 139−176.
26. Dalla Via, L., Di Noto, V., and Toninello, A. (1998) *FEBS Lett. 422*, 36−42.
27. Kroemer, G., Petit, P., Zamzami, N., Vayssiere, J. L., and Mignotte, B. (1995) *FASEB J. 9*, 1277−1287.
28. Reed, J. C., Jurgensmeier, J. M., and Matsuyama, S. (1998) *Biochim. Biophys. Acta 1366*, 127−137.
29. Cai, J., Yang, J., and Jones, D. P. (1998) *Biochim. Biophys. Acta 1366*, 139−149.
30. Susin, S. A., Zamzami, N., and Kroemer, G. (1998) *Biochim. Biophys. Acta 1366*, 151−165.
31. Lemasters, J. J., Nieminen, A. L., Qian, T., Trost, L. C., Elmore, S. P., Nishimura, Y., Crowe, R. A., Cascio, W. E., Bradham, C. A., Brenner, D. A., and Herman B. (1998) *Biochim. Biophys. Acta 1366*, 177−196.
32. Yagisawa, S. (1995) *Biochem. J. 303*, 305−311.
33. Kamo, N., Muratsugu, M., Hongoh, R., and Kobatake, Y. (1979) *J. Membr. Biol. 49*, 105−121.
34. Affolter, H., and Siegel, E. (1979) *Anal. Biochem. 97*, 315−319.
35. Jensen, B. D., Gunter, K. K., and Gunter, T. E. (1986) *Arch. Biochem. Biophys. 248*, 305−323.
36. Palmieri, F., and Klingenberg, M. (1979) *Methods Enzymol. 55*, 279−301.
37. Hille, B. (1979) in *Membrane Transport Process* (Stevens, C. F., and Tsien, R. W., Eds.) pp 5−16, Vol. 3, Raven Press, New York.
38. Stein, W. D. (1981) in *Membrane Transport* (Bonting, S. L., and de Pont, J. J. H. H. M., Eds.) pp 123−157, Vol. 2, Elsevier/North-Holland, Biomedical Press, Amsterdam, New York, Oxford.
39. Hille, B. (1984) in Ionic Channels of Excitable Membranes, Sinauer Associates Inc., Sunderland, MA.
40. Garlid, K. D., Beavis, A. D., and Ratkje, S. K. (1989) *Biochim. Biophys. Acta 976*, 109−120.
41. Gutfreund, H. (1955) *Discuss. Faraday. Soc. 20*, 167−173.
42. Anderson, O. S. (1989) *Methods Enzymol. 171*, 62−112.
43. Lauger, P. (1973) *Biochim. Biophys. Acta 311*, 423−441.

BI991217C